

Self-generated magnetic fields in laser-produced plasmas for metallic targets

David F. Edwards,* V. V. Korobkin, S. L. Motilyov, and R. V. Serov

P. N. Lebedev Physics Institute, Academy of Sciences, Moscow, USSR

(Received 19 October 1976)

Direct evidence is reported that associated with laser-produced plasma for metallic targets, the self-generated magnetic field consists of two identifiable parts having different radial and background pressure dependences as well as propagation speeds. For background pressures greater than about 0.1 mTorr and probe distances greater than 5 mm, two independent \vec{B} signals are observed. The \vec{B}_1 field is laser driven and originates from a stream of electrons ($T_e \sim 10$ eV) moving counter to the incident laser beam. The \vec{B}_2 field originates from the Korobkin effect and is associated with the expanding plasma. For the experiments reported here the magnetic fields are 10^3 G or less.

I. INTRODUCTION

The first reported measurement of self-generated magnetic fields in laser-produced plasmas was that of Korobkin and Serov.¹ They used a small induction coil to measure the presence of a magnetic moment of a laser-produced spark in air. This has subsequently been called "the Korobkin effect." Askaryan *et al.*² extended these measurements to the case of metallic targets. They measured the time rate of change of the magnetic induction, \dot{B} , produced by light pressure on the surface of a metal and in the plasma of the flare produced when a laser beam acts on a metallic surface. Since that time Stamper *et al.*,^{3,4} Serov and Richardson,⁵ Bird *et al.*,⁶ and perhaps others have performed similar experiments using different diagnostic methods, different laser frequencies, or different power levels to measure properties of these laser-produced magnetic fields. Several theoretical papers⁷⁻¹⁰ have been published in which different hypotheses are proposed as to the origin of this magnetic field and estimates are made of the magnitude of the magnetic induction, B , inside the plasma. These magnitude estimates have ranges from a few gauss to greater than a megagauss depending on the experimental parameters. As has been pointed out previously,³⁻¹⁰ megagauss fields could have a significant effect on the plasma dynamic processes as well as the momentum coupling, heating, and laser-radiation absorption properties of the laser-produced plasmas. These effects in turn could have important consequences in our understanding of the physics of laser-target interaction, in particular, the laser fusion problem.

The experiments of Stamper *et al.*³ report the radial variation of the spontaneous field to be $B \propto r^{-1.4}$ for $r < 1$ cm and $B \propto r^{-4.2}$ for $r > 1$ cm. This is for a 250- μ m-diam fiber of Lucite, and the field is observed in the plane of the fiber. Serov and Richardson,⁵ using an aluminum target,

measured an $r^{-2.1}$ radial dependence also in the plane of the target. Bird *et al.*⁶ report a field associated with the expanding front of a laser-produced plasma from an aluminum target for background gas pressures greater than 250 mTorr and distances larger than about 1 cm in front of the target. This is an azimuthal field symmetric about the laser-beam axis, and in a direction opposite to that measured with their probe near the plane of the target (distances less than about 1 cm). They do not give the radial dependence of either field. These disagreements in the measured radial dependence could be the results of different target configurations (fiber versus a flat disk), laser frequency, laser power, or some other experimental condition. In our experiments reported here we have attempted to clarify the radial dependence of the self-generated magnetic fields and to identify the source of these fields for the case of metallic targets and laser power densities 5×10^{11} W/cm² or less. From our measurements we find direct evidence that the self-generated magnetic field consists of two identifiable parts having different radial and background pressure dependences as well as different propagation speeds. From these data the origin can be identified for each of these fields.

II. EXPERIMENT

Using the experimental setup shown schematically in Fig. 1, we have measured the spatial, temporal, and background pressure dependence of the self-generated magnetic fields. The field \vec{B} was measured using a high-speed magnetic probe similar to that used originally by Korobkin and Serov¹ and is described in detail elsewhere.¹¹ The probe is an induction coil 2.6 mm in diameter with from 5 to 10 turns of 0.1-mm-diam copper wire. The coil is filled with epoxy to prevent plasma penetration and is connected to the primary of a small transformer with a grounded center tap.

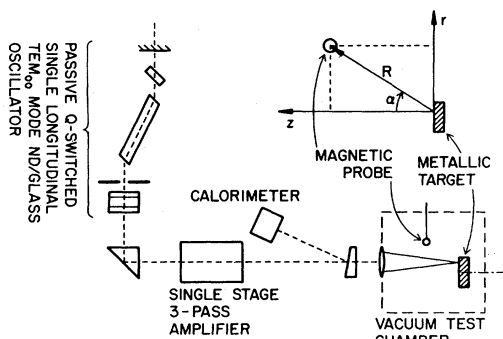


FIG. 1. Schematic sketch of the experimental setup. The Nd:glass laser is mode controlled using an aperture and a resonant cavity. The amplifier is a three-pass rod.

This construction provides a magnetic probe having a 1-nsec response and high discrimination against the various sources of electrical noise present during the creation of the laser-produced plasmas. In addition, the probe has the high sensitivity of 6 V nsec/G. The probe-amplifier combination has a signal threshold (signal-to-noise equal to unity) of 0.3 mG/nsec, and a rejection ratio (discrimination between perpendicular components of \dot{B}) greater than 10^3 . The measured rise and decay times of the magnetic probe, including cables and amplifier, is 3.5 nsec. The probe signals were consistently verified to be those of the transient magnetic induction by rotating the probe 180° and observing the accurate reversal of the signals.

A neodymium-glass laser with one stage of amplification was used to produce the plasma. The laser output was 1.2 J ($\pm 10\%$) in a 30-nsec pulse and was TEM₀₀ in a single longitudinal mode. The energy and temporal behavior were monitored for each pulse to assure the reproducible operation. The laser radiation was focused with near-normal incidence on the disk targets located inside a metallic vacuum chamber of special design. The chamber design is such that the probe-to-focal spot distance can be changed independently in the z and r directions without disturbing the focusing lens-to-target distance. Also, the target can be rotated about an axis parallel to the laser beam. This rotation of the target permits the presentation of a fresh surface to the laser beam. For a focusing lens with focal length = 20 cm, the laser spot size was estimated from burn patterns to be about 100 μm in diameter. The laser power density on target was thus of the order of 5×10^{11} W/cm². The metallic targets were disks (2 mm thick \times 20 mm diam) of iron, copper or aluminum. A disk (30 mm thick \times 20 mm diam) of insulating material, similar to Bakelite, was also

used for the reported measurements. Only data for the Fe targets are reported here. The Cu and Al data are essentially the same as that for Fe.

The temporal dependence of the \dot{B} signal was recorded for different radial and axial positions for fixed background-gas pressures. For these measurements air was the background gas. By rotating the magnetic probe, either the axial (B_z) or the azimuthal (B_ϕ) (with respect to the laser beam axis) component could be measured. For each of the measurements reported here the axial component was zero, $\dot{B}_z = 0$; the measured fields had only azimuthal components \dot{B}_ϕ .

III. EXPERIMENTAL DATA

Shown in Fig. 2 is a typical set of \dot{B} data for the case of an iron target, with background-gas pressure of 1 mTorr, and probe position $r = 1$ cm and various z values. The origin of the t axis is taken as the first maxima. For $z \sim 0.5$ cm, the \dot{B} signal is clearly seen to consist of two parts, labeled \dot{B}_1 and \dot{B}_2 . As the z position is changed, the independence of the \dot{B}_1 and \dot{B}_2 signals is demonstrated. The \dot{B}_1 signal has fast rise and decay times and a pulse width comparable to that of the laser pulse. The initiation of this pulse coincides with the time of laser-target interaction to within the temporal resolution of the measuring system (about 3.5 nsec). To first order, the pulse width of \dot{B}_1 is independent of the background pressure and is approximately that of the laser pulse. The magnitude of the \dot{B}_1 signal depends slightly on

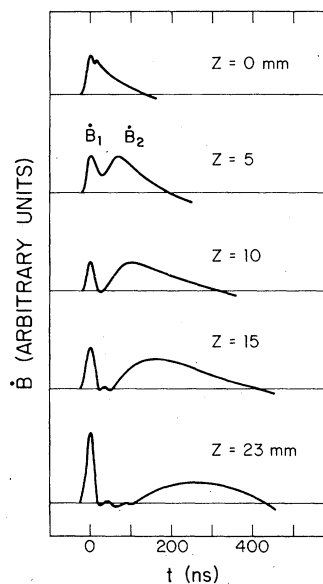
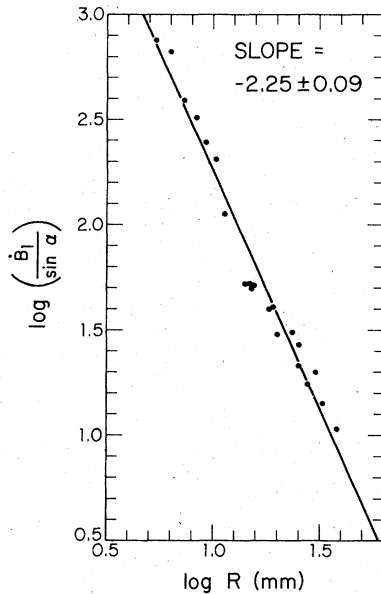


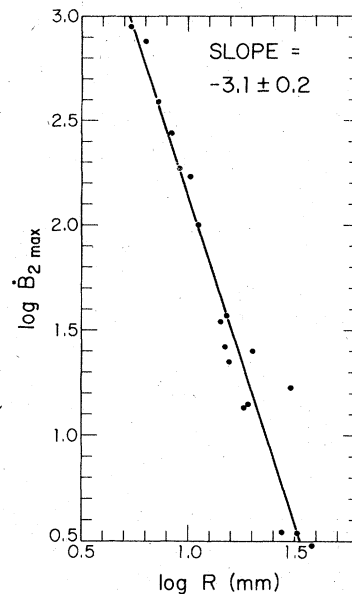
FIG. 2. Typical magnetic probe signals for background pressures of 0.1 mTorr, $r = 1$ cm and different z positions.

FIG. 3. Radial dependence of the \dot{B}_1 signal.

pressure and is discussed later. The propagation speed of the \dot{B}_1 signal is estimated to be 2×10^8 cm/sec or greater using the probe-to-laser spot distance and the $\dot{B}_{1 \max}$ time from Fig. 2. The time values from Fig. 2 and thus the propagation speeds are instrument-resolution limited but $\geq 2 \times 10^8$ cm/sec. This speed is consistent with the electron temperatures (10 eV) measured by Isenor¹² for laser-induced electron emission from metallic surfaces.

The radial dependence of \dot{B}_1 is given in Fig. 3; the straight line is a least-squares fit of the data and has the slope -2.25 ± 0.09 . In the figure, α is the angle between the z coordinate and the probe position vector, $R = (r^2 + z^2)^{1/2}$ (see Fig. 1). The \dot{B}_1 signal has only an azimuthal component ($\dot{B}_{1\phi}$) with a direction corresponding to a stream of electrons leaving the target and moving towards the focusing lens. These data indicate that the \dot{B}_1 field arises from an equivalent current element with the characteristic inverse-square radial dependence of the Biot-Savart relation. This electron current is laser driven and only exists during the laser-target interaction time. Further evidence that \dot{B}_1 arises from an electron current is found by substituting an insulating target for the metallic target. For this case the \dot{B}_1 signal is absent and only the \dot{B}_2 signal is observed. The same effect occurs when our metallic target is electrically insulated from the metal chamber; no \dot{B}_1 signal, only a \dot{B}_2 signal, is observed.

For background-gas pressures up to about 50 mTorr the propagation speed of the \dot{B}_2 signal is 2×10^7 cm/sec as estimated from the distance-

FIG. 4. Radial dependence of the \dot{B}_2 signal.

time data of Fig. 2. This is about the same speed as the initial velocity of the expanding luminous plasma of a laser-produced air spark measured by Korobkin *et al.*¹³ using an image-converter camera. The \dot{B}_2 -field radial dependence is shown in Fig. 4 where the solid line is a least-squares fit of the experimental data and has the slope -3.1 ± 0.2 . The r^{-3} behavior and the propagation speed indicate that the \dot{B}_2 field is due to the interaction of the expanding plasma and the background gas. The ion-electron separation at the front of the expanding plasma may be the source of the electric dipole. As the plasma expands from the target, this dipole changes to produce the \dot{B}_2 field. The direction of the \dot{B}_2 signal is totally azimuthal and of the same sense as the \dot{B}_1 signal.

Figure 5 shows the dependence of the magnitudes of the \dot{B}_1 and \dot{B}_2 signals on the background-gas pressure. These data are typical for the probe coordinates, $z > 2$ mm and $r > 2$ mm. As reported by Bird *et al.*,⁶ the pressure at which the \dot{B}_2 field attains the maximum value was observed to decrease as the probe distance was increased. Differences in probe distance probably account for the pressure shifts seen in comparing Fig. 5 with the data of Bird *et al.* Bird *et al.* used a metallic target insulated from the vacuum chamber and thus could not observe a \dot{B}_1 signal. They also report azimuthal fields with direction opposite to the \dot{B}_2 fields of Fig. 5 for $p > 250$ mTorr and $z > 1$ cm. Such oppositely directed fields were searched for but were not observed for our experiment, probably because Bird used larger laser peak power (300 MW vs 40 MW).

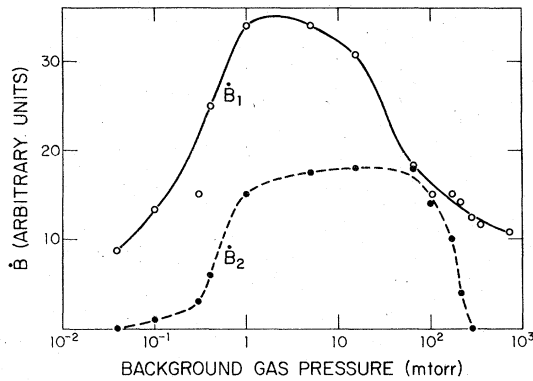


FIG. 5. The dependence of the magnitudes of the \dot{B}_1 and \dot{B}_2 signals on the background-gas pressure.

At the present time the following sources have been suggested as the origins for the magnetic fields: (a) electron and ion currents from the target, (b) charge separation in an expanding plasma, (c) temperature and density gradients in a plasma,³ (d) light pressure on a plasma,^{2,7} and (e) Faraday effect produced by circularly polarized light. For the experiments reported here, only sources (a) and (b) have significant contribution to the measured \dot{B} ; the other sources have negligible effects. Sources (a) and (b) can exist after the laser pulse

while (c), (d), and (e) can exist only in the presence of the laser pulse.

The magnitudes of the two fields, B_1 and B_2 , can be estimated by time integrating the two signals. Special attention must be paid to include only those times for B_2 before the expanding plasma has engulfed the probe. These estimates are consistent with the predictions of Widner. Experiments are currently in progress to extend these experiments to about 10^{17} W/cm² using the UMI-35 laser system under construction at the P.N. Lebedev Physics Institute. At these larger power densities, electron temperatures in excess of 10 eV are expected and, according to the calculations of Widner¹⁰ and others, sources (c), (d), and (e) are expected to be important. The resulting magnetic fields should be a megagauss or larger, according to the Widner model.

ACKNOWLEDGMENTS

The authors would like to acknowledge the stimulating discussions with Drs. G. A. Askaryan, G. Budker, and A. M. Prokhorov. One of the authors (D.F.E.) wishes to acknowledge the assistance of the Academies of Sciences of the USA and the USSR for the Visiting Scientist grant and the opportunity to participate in the Exchange Program.

*Visiting scientist from Los Alamos Scientific Laboratory, Los Alamos, New Mexico, under an exchange agreement between the National Academy of Sciences (U.S.A.) and the Academy of Sciences (USSR).

¹V. V. Korobkin and R. V. Serov, Zh. Eksp. Teor. Fiz. Pis'ma Red. **4**, 103 (1966) [JETP Lett. **4**, 70 (1966)].

²G. A. Askaryan, M. S. Rabinovich, A. D. Smirnova, and V. D. Studenov, Zh. Eksp. Teor. Pis'ma Red. **5**, 116 (1967) [JETP Lett. **5**, 93 (1967)].

³J. A. Stamper, K. Papadopoulos, R. N. Sudan, S. O. Dean, E. A. McLean, and J. M. Dawson, Phys. Rev. Lett. **26**, 1012 (1971).

⁴J. A. Stamper and B. H. Ripin, Phys. Rev. Lett. **34**, 138 (1975).

⁵R. Serov and M. C. Richardson, Appl. Phys. Lett. **28**, 115 (1976).

⁶R. S. Bird, L. L. McKee, F. Schwrizke, and A. W. Cooper, Phys. Rev. A **7**, 1328 (1973).

⁷J. A. Stamper and D. A. Tidman, Phys. Fluids **16**, 2024

(1973).

⁸J. A. Stamper, NRL Report No. 7411 (1972) (unpublished).

⁹J. B. Chase, J. L. LeBlanc, and J. R. Wilson, Phys. Fluids **16**, 1142 (1973); M. M. Widner, Sandia Report No. SLA-75-0500 (1973) (unpublished); N. K. Winsor and D. A. Tidman, Phys. Rev. Lett. **31**, 1044 (1973); L. A. Bolshov, Yu. A. Dreizin, and A. M. Dykhne, Zh. Eksp. Teor. Fiz. Pis'ma Red. **19**, 288 (1974) [JETP Lett. **19**, 168 (1974)]; A. F. Nastoyashchii, At. Energ. **38**, 27 (1975).

¹⁰M. M. Widner, Phys. Fluids **16**, 1778 (1973).

¹¹V. V. Korobkin and S. L. Motilyov (to be published).

¹²N. R. Isenor, J. Appl. Phys. **36**, 316 (1965).

¹³V. V. Korobkin, S. L. Mandelstam, P. P. Pashinin, A. V. Prokhindeev, A. M. Prokhorov, N. K. Sukhodrev, M. Ya. Schelev, Zh. Eksp. Teor. Fiz. **53**, 116 (1967) [Sov. Phys. JETP **26**, 79 (1968)].